Exfoliated Block Copolymer/Silicate Nanocomposites by One-Pot, One-Step in-Situ Living Polymerization from Silicate-Anchored Multifunctional Initiator

Jianbo Di and Dotsevi Y. Sogah*

Baker Laboratory, Department of Chemistry and Chemical Biology, Cornell University, Ithaca, New York 14853-1301

Received March 10, 2006; Revised Manuscript Received May 22, 2006

ABSTRACT: Poly(styrene-*b*-caprolactone)/silicate nanocomposites were prepared via one-pot, one-step in-situ living polymerization from a silicate-anchored bifunctional initiator. The random dispersion of the silicate layers in the polymer matrix was confirmed by both XRD and STEM. The polymer chains were attached to the surface of the silicate layers at the junction between the two blocks. SEC and NMR confirmed the block structure of the polymer. Through simultaneous incorporation of the initiator and benzyltrimethylammonium salt as a noninitiator into the silicate nanocomposites containing higher molecular weight polymers were obtained. The molecular weights of the polymers and the silicate content of the nanocomposites were also controlled. Characterization by XRD and DSC showed that the poly(caprolactone) segment existed in a crystalline state.

Introduction

Polymer silicate nanocomposites continue to see significant research effort by numerous groups, resulting in the preparation of nanocomposites containing virtually all types of polymers.[1−14] Although most of the efforts involved homopolymers,[11−14] there is interest in block copolymer silicate nanocomposites due to their higher complex structure and technological significance. However, reports on preparation of block copolymer silicate nanocomposites have been few, and the majority of the reported nanocomposites had intercalated morphology. The polymer systems include poly(styrene-*b*-butadiene-*b*-styrene) (SBS),[15] star-shaped SBS,[16] hydrogenated SBS,[17] polystyrene-*b*-poly(ethylene-*r*-butylene)-*b*-polystyrene cylindrical triblock copolymer,[18] poly(styrene-*b*-isoprene),[19,20] and poly(styrene-*b*-isoprene-*b*-styrene).[21,22] The observed morphology appeared to be independent of the method of preparation, which included melt compounding,[15,17,20] solution mixing,[16] solution mixing followed by annealing,[19,21] and solution roll casting.[22]

To increase the interaction between the polymer matrix and the silicate layers and thereby increase the probability of forming exfoliated nanocomposites, Lee et al.[23] used poly(styrene-*b*-isoprene) whose isoprene block was hydroxylated. They obtained an exfoliated nanocomposite, the formation of which they attributed to the strong attractive interactions between the hydroxyl groups of the polymer and the oxygen groups of the silicate layers. Similarly, Choi et al.[24] found that clays modified with hydroxylated surfactants dispersed well in partially hydroxylated poly(isoprene-*b*-styrene-*b*-butadiene). In the absence of the hydroxyl group on the surfactant the clay exhibited a low degree of dispersion in the same polymer. Taking a different approach, Ha et al.[25] obtained SBS/clay nanocomposites with exfoliated morphology by casting a film from solution of a mixture of SBS and oligomeric PS-modified clay prepared by "grafting from" techniques.

From a theoretical point of view, we[26] have demonstrated by molecular dynamics simulation that diblock copolymers could intercalate into layered silicates even if either or both homopolymers would not spontaneously intercalate. This was experimentally corroborated by the results of Liao et al.,[27] who used poly(ethylene-*b*-ethylene oxide) (PE-*b*-PEO) and found that not only did the PEO block intercalate into the MMT galleries but the PE block also intercalated partially although PE homopolymer would not intercalate by itself. Similar results were obtained by Gournis et al.[28] for PEO-*b*-PI/clay nanocomposites.

It is apparent from the above examples that the synthesis of block copolymer/silicate nanocomposites with exfoliated morphology has been challenging. We have recently demonstrated the effectiveness of direct synthesis of exfoliated polymer/silicate nanocomposites by in situ living free radical polymerization from silicate-anchored initiators.[29] The method permitted the control of molecular weight and polydispersity of the incorporated polymer and, more importantly, consistently gave exfoliated nanocomposites. The exfoliation was maintained even after processing, which we attributed to one end of the chain being firmly anchored to the silicate. Since then we have applied the method to the preparation of exfoliated nanocomposites containing block copolymers made by sequential monomer addition.[30] In all cases the end of one block was anchored to the silicate. Zhao et al.[31] have attempted to prepare poly(styrene-*b*-butyl acrylate)/silicate nanocomposites by in-situ sequential atom transfer radical polymerization (ATRP) from initiators immobilized within the silicate galleries of the clay particles. However, both intercalated and exfoliated silicate layers were found in their nanocomposites.

One of the technologically important uses for block copolymers is in compatibilization of polymer blends. In order for block copolymer/silicate nanocomposites to be effective in compatibilizing immiscible blends leading to novel nanocomposites with reinforced interfaces and enhanced properties, the two blocks must interact and/or form entanglements with the appropriate components of the blend. To accomplish this and at the same time fulfill the requirement that each chain be anchored to the silicate in order to effectively maintain exfoliation, we have designed a multifunctional initiator that contained a benzyltrimethylammonium group as an anchoring site and initiating sites for two different polymerization mech-

* Corresponding author. E-mail: dys2@cornell.edu.

10.1021/ma060543e CCC: $33.50
Published on Web 06/30/2006

anisms, namely, a primary alcohol functionality for living ring-opening polymerization of heterocyclic ethers and lactones and an alkoxyamine for nitroxide-mediated living free radical polymerization. By anchoring this multifunctional initiator to silicate layers and employing the previously reported one-pot simultaneous block copolymerization,[32] we expected to obtain block copolymer/silicate nanocomposites with exfoliated morphology in contrast to the intercalated structure from most of the examples discussed above. Furthermore, anchoring the block copolymer at the junction between the two blocks would make it possible for each block to more readily diffuse into and interact or entangle with a chemically similar domain in a phase-separated blend for which the block copolymer is used as a compatibilizing agent. We expect this to be more effective in compatibilizing immiscible blends and reinforcing their interfaces than would be expected from block copolymer/silicate nanocomposites in which one end of the diblock copolymer is restricted, leaving only the free end of the other block. In this paper, we describe the synthesis and the characterization of nanocomposites using one-pot, one-step in-situ block copolymerization involving simultaneous living free radical polymerization of styrene and anionic ring-opening polymerization of ϵ-caprolactone in the presence of an initiator-anchored MMT. The compatibilization studies will be reported separately.

Experimental Section

Materials. All chemicals were purchased from Aldrich and used without any further purification, unless otherwise noted. Styrene (S) (99%) and ϵ-caprolactone (CL) (99%) were distilled over CaH_2 under reduced pressure. Distilled styrene was kept over a period of no more than 2 months for use when needed while ϵ-caprolactone was used right after distillation. Tetrahydrofuran (THF) was distilled from sodium benzophenone. Na-montmorillonite silicate with a cation exchange capacity of 90 mequiv/100 g was obtained from Southern Clay Products, Gonzales, TX, and purified as described previously before use.[30] Compound **1** was synthesized following literature procedures.[33]

Characterization. X-ray diffraction (XRD) analysis was performed on powder samples with a Scintag X-ray diffractometer operating in the theta−theta geometry using Cu Kα ($\lambda = 1.54$ Å) or Cr Kα ($\lambda = 2.29$ Å) radiation operated at 45 kV and 40 mA. The scanning speed and the step size used were 5°/min and 0.02°, respectively. Room temperature solution ^{1}H nuclear magnetic resonance (NMR) spectra were obtained at 400 MHz on a VXR-400S spectrometer. Samples (25 mg) were dissolved in $CDCl_3$ (1 g) containing an internal standards of 1% TMS. Polymer molecular weights were determined from gel permeation chromatography (SEC) in THF using a Waters HPLC with Ultrastyragel (Waters Associates) columns and both refractive index and UV detectors. Retention times were converted to polymer molecular weights using a calibration curve built from narrow molecular weight distribution PS standards. Samples for differential scanning calorimetry (DSC) analysis (~5 mg) were sealed hermetically in aluminum sample pans, and DSC curves were recorded under N_2 (~50 mL/min) on a Seiko oscillating differential scanning calorimeter at a heating rate of 20 °C/min. Thermogravimetric analyses (TGA) were carried out under N_2 on a Seiko thermogravimetric differential thermal analyzer using a heating rate of 20 °C/min.

Scanning transmission electron microscopy (STEM) was done with a 100 keV HB501/UX dedicated scanning transmission electron microscope utilizing a cold field emission gun to produce a 2 Å probe, which is scanned over the specimen. The bright field and annular dark field images were digitally and simultaneously acquired and stored in standard TIFF format using a Microsoft Windows-95 based interactive graphical program WINSTEM. The specimen was prepared by grinding the bulk material mixed with 2-propanol in an Agate mortar. A holey carbon film on a copper washer was then swept through the 2-propanol, picking up numerous microscopic pieces of the material on the carbon film.

Initiator 4. Compound **1 (**3.165 g, 7.4 mmol) was dissolved in freshly distilled THF (30 mL). Then PhMgCl (2.0 M in THF, 15 mL, 30 mmol) was added dropwise. The solution was refluxed for 1.5 h upon which it turned from red to yellow. It was neutralized by adding dropwise 5% HCl aqueous solution. The solution was extracted with Et_2O three times (50 mL × 3). The organic phase was dried with Na_2SO_4 and evaporated using a rotatory evaporator to give solids that were dried in a vacuum oven. ^{1}H NMR showed peaks from both **2** and **3**. Without separating **2** from **3**, $N(CH_3)_3$/EtOH mixture (15.0 mL, 1 M, 15.0 mmol) was added to the solid, and the mixture was stirred at room temperature for 16 h. The excess $N(CH_3)_3$/EtOH was removed under vacuum with a secondary trap in line. The solid residue was washed with a mixture of CH_2Cl_2 and Et_2O (5:1, v/v), filtered, and dried. Yield: 2.22 g (78.2% based on compound **1**). ^{1}H NMR: δ ($CDCl_3$) 1.10−1.67 (m, 18H), 3.39 (s, 9H), 3.65 (m, 1H), 4.15 (dd, 1H), 5.00 (dd, 2H), 5.25 (dd, 1H), 5.60 (d, 1H), 7.41 (d, 2H), 7.62 (d, 2H).

Initiator-Modified Silicates. Purified silicate (1.5 g, 1.35 mequiv) dispersed in deionized water (200 mL) was poured into a 200 mL solution of the initiator **4** (0.54 g, 1.35 mmol) in ethanol. The mixture was kept stirring at room temperature for 24 h and filtered. The filter cake was washed with ethanol three times (10 mL × 3). The sample was kept under vacuum at 60 °C for 24 h. The yield based on the combined starting weight of purified clay and initiator **4** was around 90−95%. The initiator-modified silicate was ground into a fine powder before use.

Following the same procedure, mixtures of **4** and benzyltrimethylammonium chloride in specified molar ratios were used to prepare various initiator/noninitiator modified silicates.

A Typical Procedure for the Preparation of the Nanocomposites. To a 30 mL three-neck round-bottom flask equipped with a stirring bar were added the initiator-modified silicate (0.23 g, 0.16 mequiv initiator), styrene (2.0 mL, 17.5 mmol), hexane solution of $AlEt_3$ (0.052 mL, 1 M, 0.052 mmol), and ϵ-caprolactone (2.0 mL, 18.0 mmol). Nitrogen was bubbled into the mixture for 30 min. The mixture was stirred at 125 °C under N_2 for about 41 h. When the system was cooled to room temperature, the contents solidified. The solid was dissolved in CH_2Cl_2 (7.5 mL) and poured into methanol (10-fold excess) to precipitate the product. The solid was filtered and dried in a vacuum oven to give the product in the form of a white solid. Weight: 2.57 g. Yield: 62.6%.

Reverse Cation Exchange. To a 100 mL round-bottom flask equipped with a stirring bar and a condenser were added the nanocomposite (1.0 g), THF (50 mL), and LiBr (0.05 g). The solution was refluxed under N_2 for 24 h and filtered through Celite. The filtrate was poured into methanol (10-fold excess) to precipitate out the polymer. The polymer was filtered and dried in a vacuum oven. Weight: 0.35 g. Yield: 35.0%.

Hydrolysis of Poly(ϵ-caprolactone) Segment. A typical procedure is as follows: To a 100 mL round-bottom flask equipped with a stirring bar and a condenser were added the polymer sample from the reverse cation exchange process (1.0 g), THF (50 mL), and $(t\text{-Bu})_4NOH$ (10.0 mL, 1 M in methanol, 10.0 mmol). The solution was refluxed under N_2 for 24 h and then neutralized with 5% HCl(aq) solution to pH 7. The solution was poured into methanol (10-fold excess) to precipitate the polymer. The polymer was filtered and dried in a vacuum oven. Yield: 0.26 g.

Results and Discussion

Synthesis. The synthesis of starting material **1** was reported previously in the literature.[33] The first step gave products **2** and **3** (Scheme 1) whose separation by column chromatography proved to be tedious, leading to low yields of **2**. So the mixture of **2** and **3** were used in the subsequent reaction (without separation) to give a mixture of **3** and **4**. These were easily separated owing to the significant differences in their polarity (salt vs neutral). The isolated yield of **4** based on **1** was 78.2%.

Figure 1 shows the evolution of the XRD patterns. The *d* spacing of the unmodified silicate was 1.18 nm, which increased

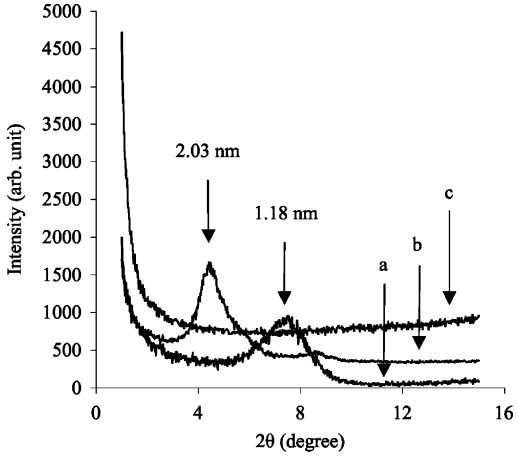

Figure 1. XRD of the unmodified silicate (a), initiator-modified silicate (b), and PS-*b*-PCL/silicate nanocomposite (c).

Scheme 1. Synthesis of the Bifunctional Initiator

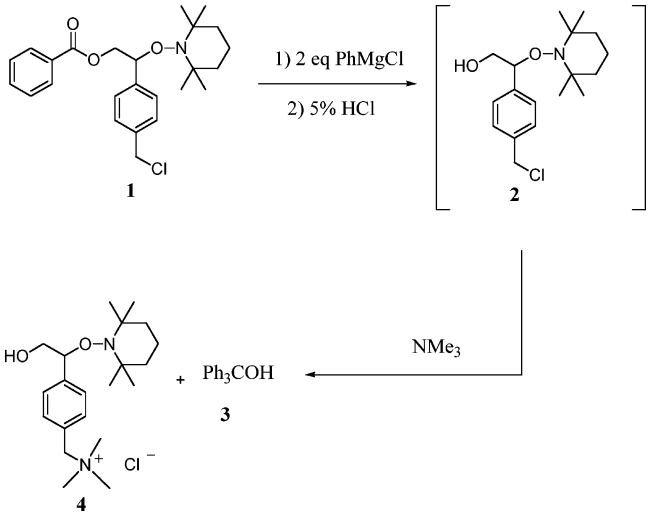

to 2.03 nm after treatment with the initiator. Besides, the peak became sharper and more symmetric. These results suggest that the initiator was anchored to the silicate to give a better defined layered structure. The small peak around $2\theta = 8.7°$ in the XRD pattern of the modified silicate is the secondary peak of the peak at $2\theta = 4.3°$.

The one-pot preparation of diblock copolymer/silicate nanocomposite is illustrated in Scheme 2. The free radical polymerization and anionic ring-opening polymerization were shown previously not to interfere with each other and, hence, could proceed simultaneously in the same reactor. However, the studies showed that polymerization of CL reached high conversion within 20 min while the free radical polymerization of styrene took 7−20 h. Table 1 shows the series of block copolymer silicate nanocomposites prepared. The result showed that at lower molecular weights the observed M_n's were closer to the calculated ones, and the polydispersity index was controlled below 1.7 up to $M_n = 94\,000$ (**1a**−**1d**). The broader than expected molecular weight distributions might be due to inadequate kinetic control and transesterification, which was previously demonstrated for the simultaneous copolymerization of CL and styrene in the absence of clay.[32] The molecular weight increased with decreasing silicate content as expected. Although the two monomers were added in equal mole ratios, the PCL block length (degree of polymerization) was about twice the PS block length in the isolated copolymers. We attribute this to the fact that polymerization of CL was faster and completed long before styrene polymerized. This would lead to the mixture becoming very viscous, which in turn would decrease the probability for the polymerization of styrene to go to higher conversions. Any unreacted monomer was essentially styrene.

For all the nanocomposites (**1a**, **1b**), the XRD showed no peaks, indicating the disorder/dispersion of the silicate layers in the polymer matrix. A typical XRD of the nanocomposites is given in Figure 1. This was further supported by STEM (Figure 2), which showed clearly that the silicate layers were dispersed into single layers (dark lines) and oriented randomly in the polymer matrix.

To provide evidence for the block structure and determine the extent to which other characteristics were controlled, the polymer was desorbed from the silicate in a reverse cation exchange by refluxing the nanocomposite in a THF solution of LiBr. To determine whether the condition of the reverse cation exchange introduced any change into the polymer structure, pure PS-*b*-PCL independently prepared was put through the same process as a control. Neither SEC nor NMR of the resulting polymer showed any difference from those of the starting material. The ^{1}H NMR of the desorbed polymer (Figure 3a) showed signals typical for the PS and PCL blocks. In addition, SEC analysis showed unimodal molecular weight distributions. To confirm the formation of the block copolymer, **1c** was hydrolyzed with a strong base to give PS. The ^{1}H NMR (Figure 3b) clearly showed complete disappearance of the PCL block while SEC showed a decrease in molecular weight and gave PDI = 1.21. These results are consistent with the formation of a block copolymer. The lower PDI suggests that the initial broader MWD was indeed due to the PCL block which formed very early in the reaction and probably underwent transesterification during the high-temperature styrene polymerization.

Control of the Molecular Weight and Silicate Content. A major advantage provided by nanocomposites resides in their enhanced properties at relatively low (5%) inorganic content. In addition, high molecular weight polymers are needed to achieve useful physical and thermal properties. However, as shown in Table 1, the higher the molecular weight of the polymer was, the lower the weight percentage of the inorganic content. This is because molecular weight is controlled by the molar ratio of monomer to initiator. Since the initiator is attached to the silicate, high molecular weight will require low initiator and hence low silicate content. To get around this conundrum, a noninitiating salt, benzyltrimethylammonium chloride, was used to replace a fraction of the initiator during the preparation of the initiator-modified silicate. The total number of moles of the initiator and noninitiator salt was equal to the total cation exchange capacity of the silicate used. This dilution would permit lowering the amount of initiator without lowering the silicate content. This technique provides a way to tailor grafting density, molecular weight, and clay content to both research and application needs. We have independently shown through separate experimentation that the ion exchange selectivities of the two ammonium salts are approximately the same.

Table 2 shows the *d* spacings of the various initiator/noninitiator-modified silicates. The *d* spacing of the original silicate was 1.18 nm. Modification separately with 100% initiator and 100% noninitiator gave *d* spacings of 2.04 and 1.47 nm, respectively. When the relative amount of the initiator in the mixture decreased, the *d* spacing of the resulting modified silicate decreased toward the value of the 100% noninitiator-modified silicate. At or below 50 mol % initiator content the *d* spacing remained constant at the value for the noninitiator-modified silicate. This suggests that at low percentage of the

Scheme 2. Diblock Copolymer/Silicate Nanocomposites from Silicate-Anchored Bifunctional Initiators

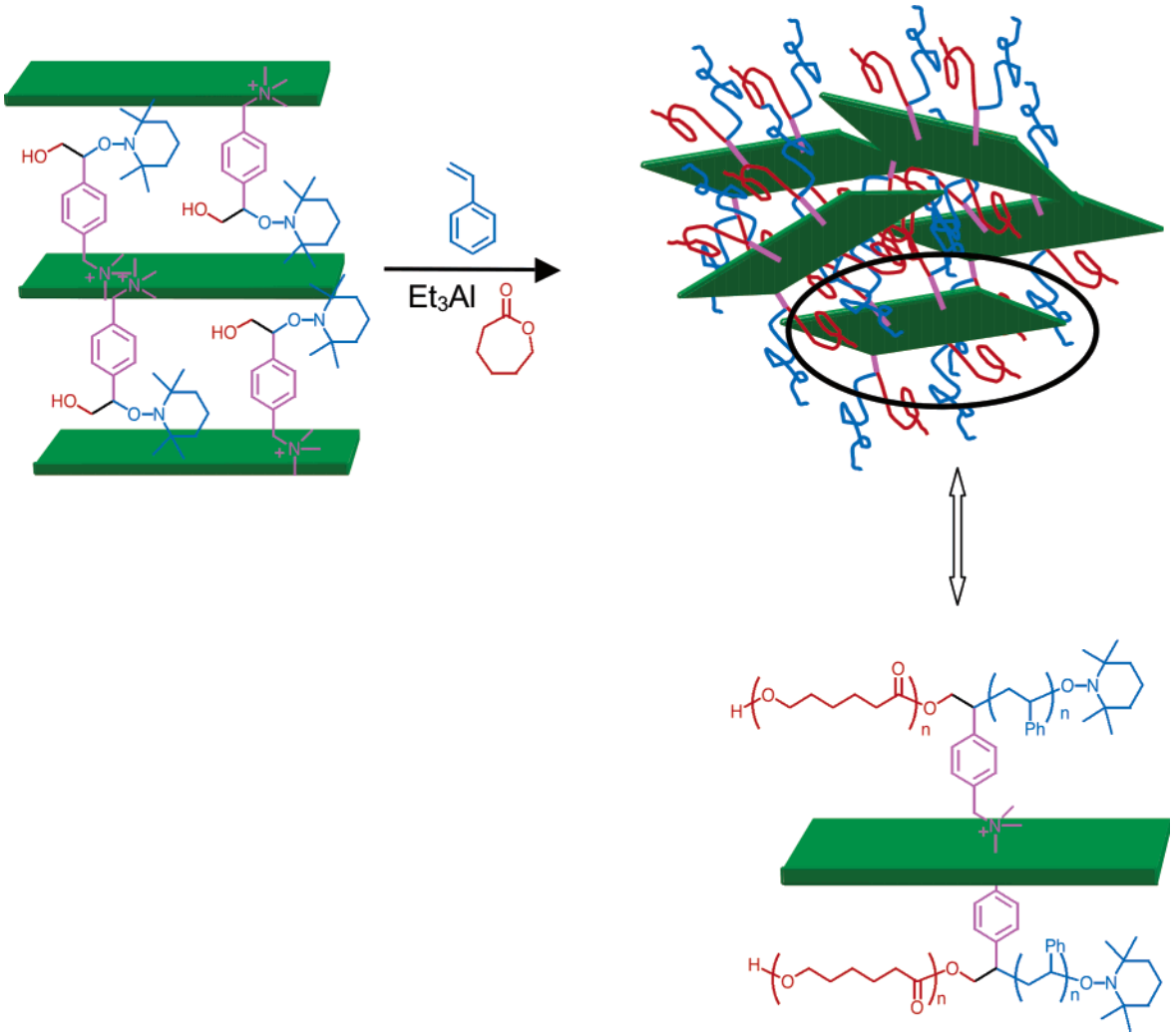

Table 1. Characterization of PS-*b*-PCL/Silicate Nanocomposites

run[a]	S[b] (equiv)	CL[b] (equiv)	M_n[c] (calc) × 10^{-3}	M_n[d] (SEC) × 10^{-3}	PDI[d]	yield (%)	S:CL[e] from NMR	silicate[f] weight (%)
1a	110	110	14.9	13.8	1.41	62.6	0.35/0.65	6.3
1b	280	280	45.4	31.2	1.32	73.1	0.29/0.71	3.4
1c	510	520	67.1	44.3	1.56	60.2	0.37/0.63	3.2
1d	990	1020	131.2	93.7	1.69	59.7	0.31/0.69	0.4
2a	1140	1180	180.2	126.5	2.69	71.5	0.37/0.63	1.0
3a	620	640	96.7	50.2	1.63	67.8	0.35/0.65	0.6
3b	1380	1430	191.5	113.6	2.28	62.5	0.34/0.66	0.2

[a] **1a**−**1d** were prepared using the 100% initiator-modified silicate, **2a** was prepared using 50/50 initiator/noninitiator-modified silicate, and **3a** and **3b** were prepared using 30/70 initiator/noninitiator-modified silicate. [b] Molar equivalents of each monomer with respect to initiating sites. [c] Calculated value based on monomer conversion and equivalent of initiator sites. [d] Determined by SEC. [e] Copolymer composition determined by NMR. [f] Determined by TGA.

initiator it could exist in a bent or inclined conformation, which would reduce its effective size. Consequently, the intergallery expansion was dominated by the noninitiator.

The 50/50 initiator/noninitiator-modified silicate was used to prepare the nanocomposite **2a** (Table 1). Molecular weight as high as 126 000 were achieved. XRD showed no peak. However, when the 30/70 initiator/noninitiator-modified silicate was used to prepare the nanocomposites **3a** and **3b**, the XRD for both showed a peak at the same position as the peak seen for the corresponding initiator/noninitiator-modified silicate. This suggests that at the high relative amount of the noninitiator some of the silicate was modified with only the noninitiator, which remained unreacted.

Figure 4 shows the typical DSC plot for the nanocomposites. It showed the melting point of the PCL segment at 56 °C (literature[34] value 56.8 °C), indicating that the PCL segment remained in the crystalline state. However, DSC did not detect the T_g of either PCL block or PS block. The XRD of the nanocomposites showed diffraction peaks corresponding to the crystalline structure of PCL segment at $2\theta = 21.5°$ and 23.8° (Figure 5).[34]

Scheme 3 illustrates a diagrammatic representation of the structure of the diblock copolymer/silicate nanocomposite. On the basis of our knowledge of the mechanism of the reaction and the fact that the initiator was preattached to the silicate layers, we concluded that the polymer chains were attached to the silicate at the junction of the two blocks with free ends of the PS and the PCL blocks. This conclusion is supported by the fact that all the characterization methods we employed did not reveal the presence of unattached chains. The polymer

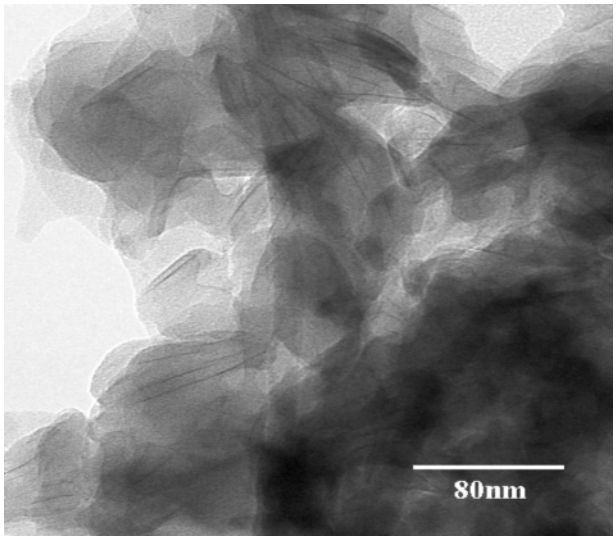

Figure 2. STEM image of PS-*b*-PCL/silicate nanocomposite (**1a**, Table 1**)**.

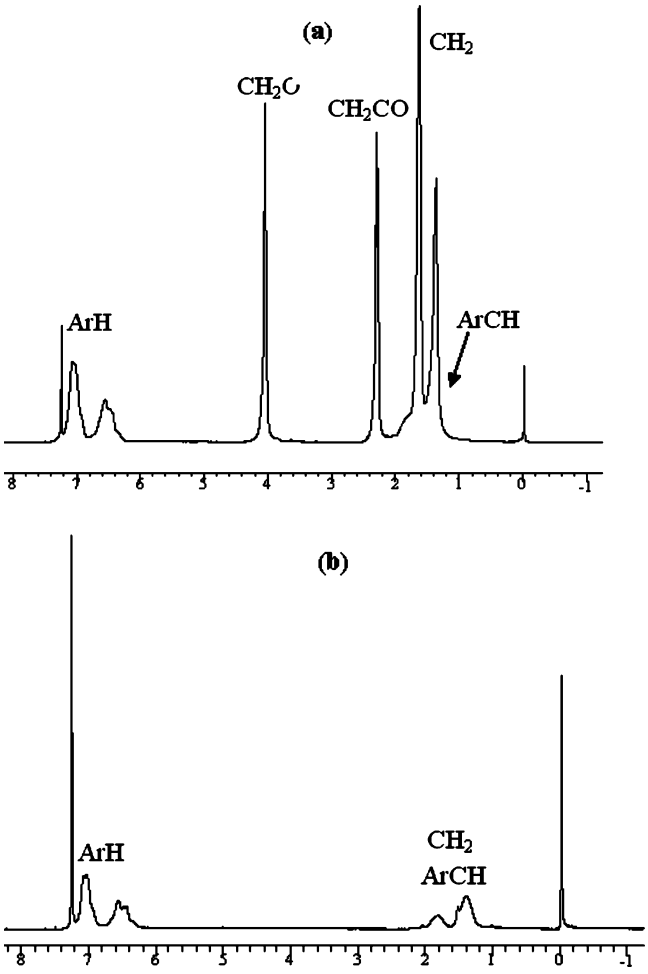

Figure 3. ^{1}H NMR of polymer **1c** (a) and its hydrolysis product (b).

removed from the nanocomposite by reverse ion exchange was clearly shown to be a block copolymer based on the observation that (1) there was a reduction in the GPC molecular weight as PCL segment was hydrolyzed off, (2) the NMR, GPC, and X-ray diffraction showed the material to be identical to an authentic independently synthesized block copolymer, and (3) GPC did not show any peaks due to free polymer, which we would have seen because the molecular weight would be different from that of the block copolymer. These suggest that if any free polymer

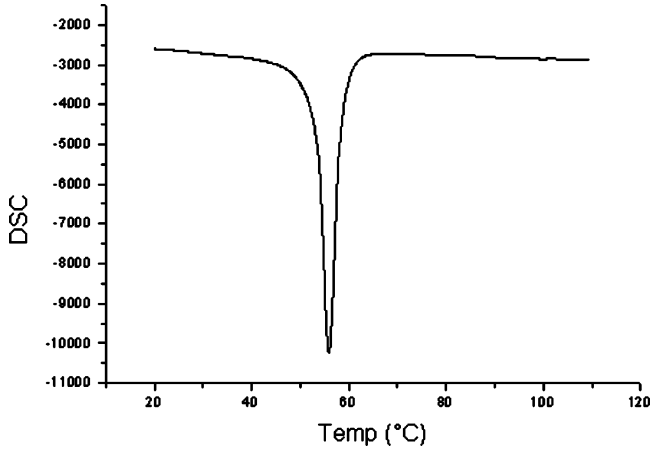

Figure 4. DSC on the nanocomposite showing the T_m of the PCL segment.

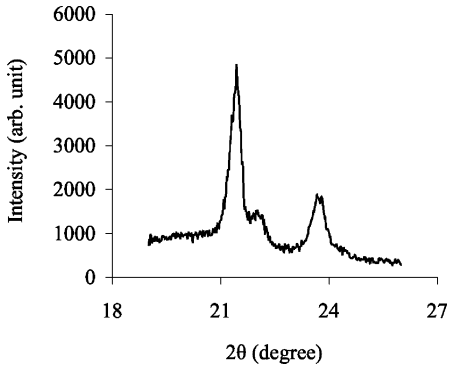

Figure 5. XRD of the nanocomposites showing diffraction peaks corresponding to the crystalline structure of the PCL segment at $2\theta = 21.5°$ and 23.8°.

Table 2. X-ray Diffraction Angle and *d* Spacing of Initiator/ Noninitiator-Modified Silicate

feed initiator/ noninitiator molar ratio	2θ (deg)	*d* spacing (nm)
100/0	4.33	2.03
70/30	5.88	1.50
50/50	6.02	1.47
30/70	6.02	1.47
0/100	6.02	1.47
pure silicate	7.48	1.18

Scheme 3. Illustration of the Structure of the Diblock Copolymer Silicate Nanocomposites[a]

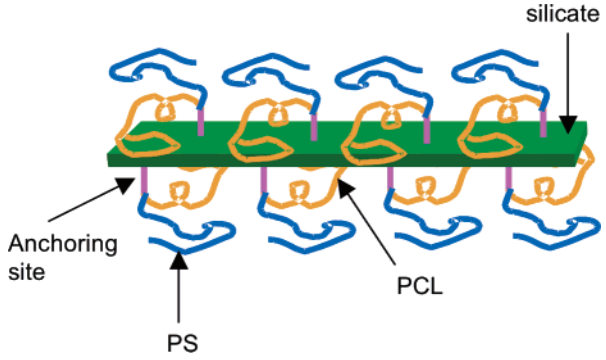

[a] The polymer chains are attached to the silicate layers at the junctions of the diblock copolymer with both chain ends left free.

was produced as a result of thermal polymerization of styrene or backbiting in PCL, which would lead to unattached cyclic oligomers, it was in an insignificant amount, which was probably washed off during isolation and purification of the nanocom-

posite. Considering the much larger dimensions of the silicate layers, the phase-separated nature of PCL and PS due to their immiscibility, and the higher polarity of PCL than PS, we propose a structure in which the crystalline PCL remained close to the surface of the silicate layers with the amorphous PS surrounding the outside (Scheme 3). This unique characteristic provides the potential for using the nanocomposite as a compatibilizing agent for either PS/PCL blends or other blends with which PS and PCL are respectively miscible. The method should facilitate the development of other block copolymer nanocomposites as compatibilizing agents in immiscible blends.

Summary

Poly(styrene-*b*-caprolactone)/silicate nanocomposite was prepared via one-pot, one-step in-situ living polymerization from a silicate anchored bifunctional initiator. The random dispersion of the silicate layers in the polymer matrix was confirmed by both XRD and STEM. The polymer chains were attached to the surface of the silicate layers at the junctions between the two blocks. SEC and NMR confirmed the block structure of the polymer. By diluting the initiator with a noninitiating salt, a relatively high molecular weight of the polymer was obtained while a certain inorganic weight percentage was maintained. Preliminary study of the nanocomposite by XRD and DSC showed that the PCL segment existed in a crystalline state.

Acknowledgment. This research was funded by NSF under Grant DMF-0079992 and DuPont Company through Polymer Outreach Program of Cornell Center for Materials Research. Particular acknowledgment is made of the use of the XRD, STEM, SEC, TGA, and DSC Facilities of the CCMR. The STEM laboratory is supported by the Cornell Center for Materials Research (NSF DMR-9632275). The HB501 UHV-STEM was acquired through the National Science Foundation (Grant DMR-8314255). The authors thank Mr. Mick Thomas for the help with STEM measurements and Dr. Maura Weathers for help with XRD tests. The authors acknowledge the help from Dr. Marc Weimer with the project.

References and Notes

(1) Vaia, R. A.; Jandt, K. D.; Kramer, E. J.; Giannelis, E. P. *Macromolecules* **1995**, *28*, 8080−8085.
(2) Shi, H.; Lan, T.; Pinnavaia, T. J. *Chem. Mater.* **1996**, *8*, 1584−1587.
(3) Vaia, R. A.; Giannelis, E. P. *Macromolecules* **1997**, *30*, 7990−7999.
(4) Vaia, R. A.; Giannelis, E. P. *Macromolecules* **1997**, *30*, 8000−8009.
(5) Lyatskaya, Y.; Balazs, A. C. *Macromolecules* **1998**, *31*, 6676−6680.
(6) Zhulina, E.; Singh, C.; Balazs, A. C. *Langmuir* **1999**, *15*, 3935−3943.
(7) Pinnavaia, T. J. *Science* **1983**, *220*, 365−71.
(8) Yano, K.; Usuki, A.; Okada, A.; Kurauchi, T.; Kamigaito, O. *J. Polym. Sci., Part A: Polym. Chem.* **1993**, *31*, 2493−8.
(9) Lan, T.; Kaviratna, P. D.; Pinnavaia, T. J. *Chem. Mater.* **1994**, *6*, 573−5.
(10) Okada, A.; Kawasumi, M.; Usuki, A.; Kojima, Y.; Kurauchi, T.; Kamigaito, O. *Mater. Res. Soc. Symp. Proc.* **1990**, *171*, 45−50.
(11) Krishnamoorti, R.; Giannelis, E. P. *Macromolecules* **1997**, *30*, 4097−4102.
(12) Kornmann, X.; Berglund, L. A.; Skerte, J.; Giannelis, E. P. *Polym. Eng. Sci.* **1998**, *38*, 1351−1358.
(13) Giannelis, E. P. *Appl. Organomet. Chem.* **1998**, *12*, 675−680.
(14) Giannelis, E. P. *Adv. Mater.* **1996**, *8*, 29−35.
(15) Laus, M.; Francescangeli, O.; Sandrolini, F. *J. Mater. Res.* **1997**, *12*, 3134−3139.
(16) Liao, M.; Zhu, J.; Xu, H.; Li, Y.; Shan, W. *J. Appl. Polym. Sci.* **2004**, *92*, 3430−3434.
(17) Hasegawa, N.; Usuki, A. *Polym. Bull. (Berlin)* **2003**, *51*, 77−83.
(18) Lim, S. T.; Lee, C. H.; Kwon, Y. K.; Choi, H. J. *J. Macromol. Sci., Phys.* **2004**, *B43*, 577−589.
(19) Ren, J.; Silva, A. S.; Krishnamoorti, R. *Macromolecules* **2000**, *33*, 3739−3746.
(20) Chen, H.; Schmidt, D. F.; Pitsikalis, M.; Hadjichristidis, N.; Zhang, Y.; Wiesner, U.; Giannelis, E. P. *J. Polym. Sci., Part B: Polym. Phys.* **2003**, *41*, 3264−3271.
(21) Lee, J. Y.; Park, M. S.; Yang, H. C.; Cho, K.; Kim, J. K. *Polymer* **2003**, *44*, 1705−1710.
(22) Ha, Y.-H.; Thomas, E. L. *Macromolecules* **2002**, *35*, 4419−4428.
(23) Lee, K. M.; Han, C. D. *Macromolecules* **2003**, *36*, 804−815.
(24) Choi, S.; Lee, K. M.; Han, C. D. *Macromolecules* **2004**, *37*, 7649−7662.
(25) Ha, Y.-H.; Kwon, Y.; Breiner, T.; Chan, E. P.; Tzianetopoulou, T.; Cohen, R. E.; Boyce, M. C.; Thomas, E. L. *Macromolecules* **2005**, *38*, 5170−5179.
(26) Lee, J. Y.; Baljon, A. R. C.; Sogah, D. Y.; Loring, R. F. *J. Chem. Phys.* **2000**, *112*, 9112−9119.
(27) Liao, B.; Song, M.; Liang, H.; Pang, Y. *Polymer* **2001**, *42*, 10007−10011.
(28) Gournis, D.; Floudas, G. *Chem. Mater.* **2004**, *16*, 1686−1692.
(29) Weimer, M. W.; Chen, H.; Giannelis, E. P.; Sogah, D. Y. *J. Am. Chem. Soc.* **1999**, *121*, 1615−1616.
(30) Di, J.; Sogah, D. Y. *Macromolecules* **2006**, *39*, 1020−1028.
(31) (a) Zhao, H.; Farrell, B. P.; Shipp, D. A. *Polymer* **2004**, *45*, 4473−4481. (b) Zhao, H.; Shipp, D. A. *Chem. Mater.* **2003**, *15*, 2693−2695.
(32) (a) Weimer, M. W.; Scherman, O. A.; Sogah, D. Y. *Macromolecules* **1998**, *31*, 8425−8428. (b) Sogah, D. Y.; Weimer, M. W.; Scherman, O. A. *Polym. Mater. Sci. Eng.* **1999**, *80*, 86−87. (c) Hawker, C. J.; Hedrick, J. L.; Malmström, K. E.; Trollsas, M.; Mercerreyes, D.; Moineau, G.; Dubois, P.; Jérôme, R. *Macromolecules* **1998**, *31*, 213−219. (d) Mercerreyes, D.; Moineau, G.; Dubois, P.; Jérôme, R.; Hedrick, J. L.; Hawker, C. J.; Malmström, K. E.; Trollsas, M. *Angew. Chem., Int. Ed.* **1998**, *37*, 1274−1276.
(33) Puts, R. D.; Sogah, D. Y. *Macromolecules* **1997**, *30*, 7050−7055.
(34) Wu, T.-M.; Cheng, J.-C.; Yan, M.-C. *Polymer* **2003**, *44*, 2553−2562.

MA060543E